Zero Carrier Velocity Induced Quantum Criticality in $NbFe_2$

Brian Neal, Erik R. Ylvisaker, and Warren E. Pickett
Department of Physics, University of California Davis
(Dated: June 2, 2010)

PACS numbers:

Quantum phase transitions, and the quantum critical (QC) behavior displayed near these transitions, arise from quantum fluctuations, which involve the lowest energy excitations of the material. In metals, these excitations lie at the Fermi surface, and require some peculiar feature of the Fermi surface or the related near-zero-energy fluctuations to drive the transition and to give rise to the quantum critical fluctuations around the critical point. A number of quantum critical materials have been discovered experimentally and in some cases have been studied in great detail. Rarely has any Fermi surface feature been identified as clearly responsible for quantum criticality, possibly because most QC metals are strongly correlated systems whose Fermi surfaces, hence their low energy band structures, are not given precisely enough by the available mean field band theories and material-specific self-energy corrections. The transition metal intermetallic compound $NbFe_2$ is more likely than f-electron materials or doped correlated insulators to be described accurately with moderately correlated approaches. In this QC compound we obtain an obvious candidate for the origin of quantum criticality: an accidental Fermi surface "hot stripe" corresponding to a vanishing quasiparticle velocity on the Fermi surface at an unconventional band critical point (uBCP) of $NbFe_2$, which can be accessed by tuning the stoichiometry.

$Nb_{1-x}Fe_{2+x}$ is a rare example of an itinerant transition metal intermetallic compound displaying antiferromagnetic quantum criticality. Its unusual magnetic behavior and its sensitivity to off-stoichiometry (Nb deficiency x) has been known for over two decades,[1,2] and its phase diagram and low temperature (T), small x behavior has recently been clarified.[3–5] At stoichiometry, its susceptibility is Curie-Weiss-like down to the SDW transition (probably long wavelength) at T_{sdw}=10 K with vanishing Curie-Weiss temperature, reflecting antiferromagnetism (AF) in close proximity to a FM QCP. Strongly negative magnetoresistance and a metamagnetic transition around 0.5 Tesla (at 2 K) reflect the removal of strong magnetic fluctuations by a relatively small field. The QCP occurs at the small Nb excess of x_{cr} = -0.015, for which resistivity scaling as $T^{1.5}$ and linear specific heat coefficient $\gamma \propto \ln T$ below 4 K reflect non-Fermi liquid behavior characteristic of a QCP. Even off stoichiometry the samples are rather clean (residual resistivity as low as[4] 5 $\mu\Omega$ cm). For $x < x_{cr}$ and for $x > 0.008$, ferromagnetic (FM) (including possibly ferrimagnetic [FiM]) order is observed.[4] This system has been featured in recent overviews of quantum criticality in weak magnets[6,7] and that in searching for the mechanism of quantum criticality more emphasis should be given to transition metal compounds[8] (versus f-electron systems).

There is no viable explanation of why this particular itinerant system should display such unusual quantum criticality, and this is the question we address here. The most detailed theories of quantum criticality suppose that the physics is dominated by fluctuations around the critical point, and treat the effects of low energy fermionic excitations without specifically addressing their origin.[9–13] The shortcomings of current theories for itinerant quantum criticality have been re-emphasized recently.[14] A necessary assumption is an underlying well

behaved non-interacting fermionic system. Imada *et al.*[15] have suggested itinerant quantum criticality arises either from proximity to a first-order transition (quantum tricriticality), a metal-insulator transition (which is not the case here), or a Lifshitz transition, which accompanies a change in topology of the Fermi surface. Frustration of magnetic order on the Fe2 Kagome sublattice has also been suggested as playing a part.[16] The study of interacting systems near conventional BCPs (van Hove singularities) indicates non-Fermi liquid behavior[17] and a profusion of possible phases.[18] Stronger singularities may be expected to further complicate the phase diagram.

$NbFe_2 \equiv NbFe1_{0.5}Fe2_{1.5}$ forms in the hexagonal Laves phase C14 space group $P6_3/mmc$ (#194), with Nb at $4f$ ($\frac{1}{3}, \frac{2}{3}, u$) which can be considered to lie within Fe cages, Fe1 at $2a$ (0,0,0) which lies on a hexagonal sublattice, and Fe2 at $6h$ (v,$2v$,$\frac{3}{4}$) sites that form Kagome lattice sheets in the basal plane. We perform all calculations with the experimental lattice constants a=4.841$\mathring{A}$, c=7.897$\mathring{A}$, and relaxed internal parameters u=0.0652, v=0.1705.

The complex band structure (due to 12 transition metal atoms in the unit cell) is shown in a 2 eV region centered on the Fermi energy (E_F) in Fig. 1. The Fermi surfaces are correspondingly many and varied. The point to note is the wiggle in the band just crossing E_F along the Γ-M direction that produces an unusually flat portion only 6 meV (equivalent to 70 K temperature) above E_F. This critical region produces electronic excitations that can account for anomalous behavior, *viz.* a quantum critical point at a low doping level, as is observed in $NbFe_2$ (x_{cr} = -0.015), which is the point we return to below.

Referencing the energy and wavevector to the point of the anomaly, the uBCP dispersion is given to lowest order along each axis by

$$\varepsilon_k = \frac{1}{3m_e\kappa}k_x^3 + \frac{k_y^2}{2m_y} - \frac{k_z^2}{2m_z}, \tag{1}$$

i.e. it is effective-mass-like along k_y and k_z with opposite signs of the masses m_y, m_z, but it is infinitely massive along the k_x direction, with cubic rather than quadratic variation. (The calculated band is even flatter than this approximation.) We characterize this dispersion through the wavevector κ, corresponding heuristically to a mass suppression k_x/κ. The crossing bands have nearly pure Fe2 d_{xz}, d_{yz} character (the Kagome sublattice), not involving either Fe1 or Nb orbitals.

This anomalous dispersion is an accidental occurrence (not related to symmetry or normal band edges), resulting from the crossing of two bands that occurs extremely near the Fermi level of stoichiometric $NbFe_2$. Its distinctive character is evident by noting that the change in the constant energy surfaces near E=0 does not fit into the conventional categorization.[19] Because it is accidental, it requires tuning to put E_F exactly at the critical point, and the value x_{cr} of $NbFe_2$ is of the right magnitude to provide this tuning [N(E_F)× 6 meV = 0.02 electrons/f.u.]. Although alloy calculations can determine in systems such as this how the Fermi energy will move with concentration, to do so at such small value of x_{cr} is a considerable numerical challenge beyond the scope of this paper. We pursue the scenario that Nb doping to x_{cr} places E_F at this critical value, and begin to examine the consequences.

The Fermi energy E_F lies in a region of steeply decreasing density of states (DOS) (the full DOS has been presented by Takayama and Shimizu[20] and by Subedi and Singh (SS)[21]), corresponding to the gaps that open in much of the zone (along K-H, along L-H-A). The DOS near E_F is displayed in Figure 2 and gives an idea of the magnitude of the peak at the uBCP; the form is given more precisely in the inset.

We first explore magnetic tendencies and the distribution of moments in $NbFe_2$ by performing fixed spin moment calculations. The energies and atomic moments are presented in Fig. 4. Because in the absence of constraints the nonmagnetic state is calculated to

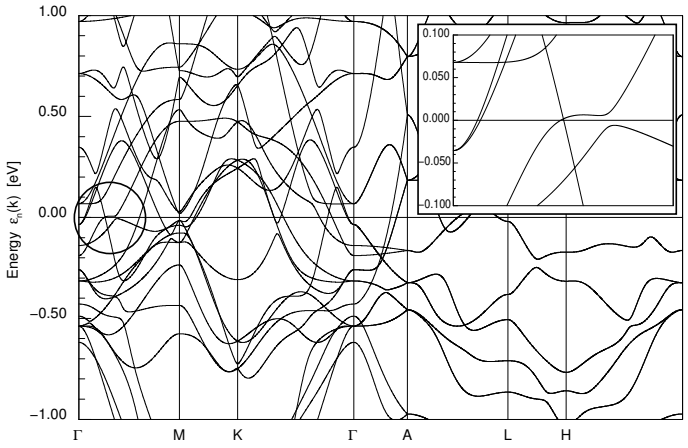

FIG. 1: Band structure of $NbFe_2$ within 1 eV of the Fermi level. The inset shows the band critical point 6 meV above E_F that lies one-third of the way along the Γ-M line.

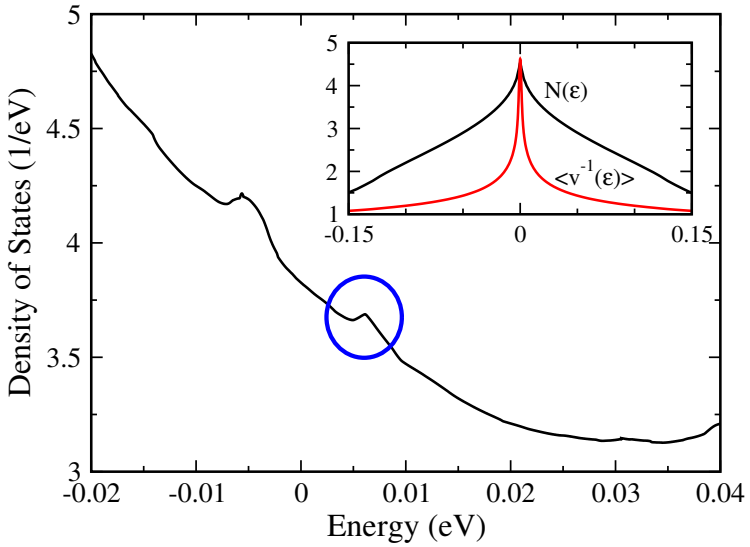

FIG. 2: The DOS of $NbFe_2$ near E_F on a fine scale, showing the steeply decreasing DOS in the region of E_F. The circle indicates the position in energy of the uBCP, 6 meV above E_F, calculated without the precision necessary to establish the shape of the anomaly. The inset shows a high resolution calculation (in arbitrary units) in the uBCP region of the behavior of N(E) (black curve), and indicating the divergence of the inverse velocity $< v^{-1}(E) >$ (red curve), which is a fundamental quantity in Moriya's theory of weak magnetism.

be unstable to magnetic order (as observed), the curves are not symmetric around zero moment; however, there is a symmetry related solution at negative M where all spin directions are reversed. Two magnetic states are evident, a low net moment ferrimagnetic (FiM) arrangement and a ferromagnetic (FM) state. The more stable state is the FiM one with total moment of 0.4 μ_B (all moments are quoted per formula unit), comprised of moments of about 1 μ_B on Fe2 and -1.8 μ_B on Fe1. For the range studied there is always a small negative moment (of the order of 0.1 μ_B) or less) on the Nb atom. (Recall the atomic ratios

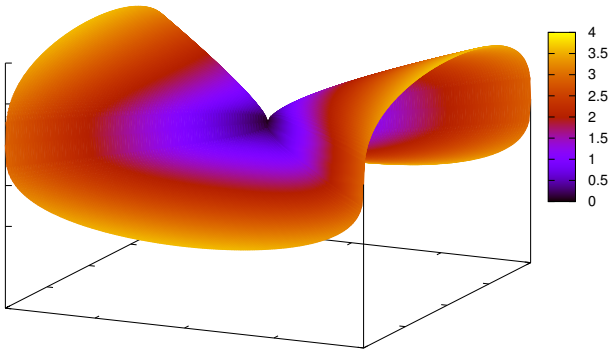

FIG. 3: Fermi surface (constant energy E=0) around the uBCP (see text), which lies at the center of the plot where the velocity vanishes; the anomalous k_x direction is plotted vertically. The color map indicates the relative velocity; the $\vec{k}$, energy, and velocity scales are arbitrary.

are $NbFe1_{0.5}Fe2_{1.5}$.) As the imposed total moment is increased, the moments on both Fe atoms initially change by comparable amounts (but of course change in opposite directions). In the region of M=1.4 μ_B the small downward moment of Fe1 becomes unstable, and it flips direction in a first-order fashion to the FM state, where it rapidly approaches the same moment as Fe2. The minimum energy of the FM state (2.4 μ_B) occurs with moments of about 1.1 μ_B and 1.5 μ_B on the Fe1 and Fe2 atoms respectively. The energy is 120 meV/f.u. higher than the FiM state. The strong variation in moments with applied field indicates itinerant character of the magnetism, in agreement with the conclusion of SS. SS obtained five types of magnetic solutions, all with much larger moments than seen experimentally (as are ours), which (independently of the quantum criticality) points to the dominating influence of magnetic fluctuations.

The FSM calculations, and the results of SS, establish there are many ordered collinear states at stoichiometry differing in energy by only $\sim$ 100 meV/f.u.. Unlike in fluctuating systems, magnetism in mean field approximation (as from DFT calculations with static moments) is not very sensitive to small anomalies in the band structure, and FSM results at x_{cr} show little difference. The near degeneracy of two several magnetic states, as well as the possibility of magnetic frustration on the Kagome Fe2 sublattice, raises the possibility of non-collinear magnetism (*i.e.* SDW) as well. Such behavior can depend on the (complicated) FSs, but SS found a relatively weak variation of the generalized susceptibility in $NbFe_2$. We do not pursue noncollinear magnetism here, but proceed to analyze the implications of the uBCP that can be accessed by as little as 6 meV change in the chemical potential.

The occurrence of BCPs (vanishing velocity) was first studied systematically by van Hove,[22] who noted that in the absence of restrictions BCPs in a band occur at most as isolated points. He studied the conventional (cBCP) case where the determinant of the Hessian $\nabla_k \nabla_k \varepsilon_k$ evaluated at the BCP is non-vanishing, which corresponds to vanishing velocity at (1) band edges, where the constant energy surface also vanishes, and (2) saddle points, with $\vec{v} = 0$ on a pinched-off surface. For our representation of the uBCP in $NbFe_2$, this *determinant vanishes* due to the cubic variation with k_x, resulting in this unconventional

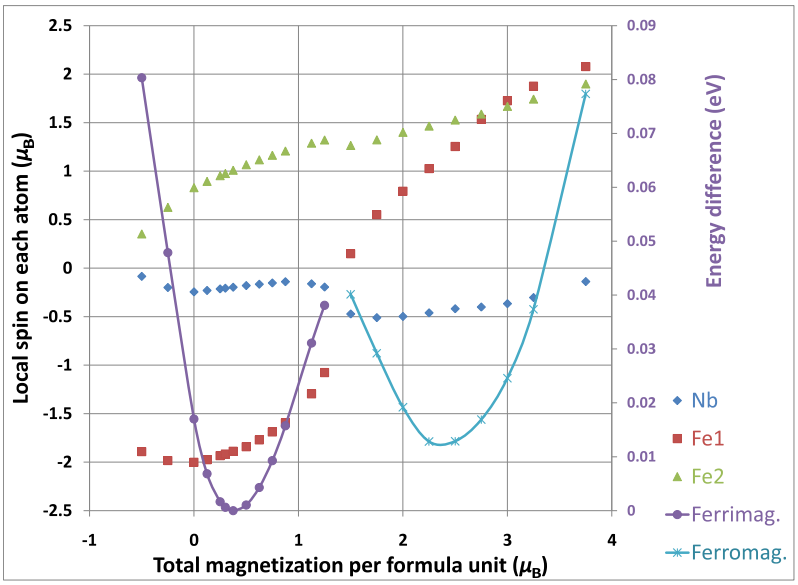

FIG. 4: Atomic moments (symbols) and energies (solid lines) from fixed spin moment studies, showing two distinct phases, ferrimagnetic (FiM) with minimum of energy around 0.3 μ_B/f.u., and ferromagnetic (FM) with minimum at 2.3 mu_B/f.u. The minima differ by 130 meV/f.u. Here M=0 corresponds to a zero moment ferrimagnetic state, hence the curve is not symmetric around M=0.

type of BCP. This uBCP therefore does not correspond to the usual possibilities, which are a (dis)appearing of a Fermi surface or to a pinching off of the Fermi surface. Instead, it is an isolated vanishing of carrier velocity on an extended surface, which is shown in Fig. 3. A spectrum of soft excitations (arbitrarily low velocities on the Fermi surface) vanishing more conventionally (linearly) in the k_y and k_z directions is joined by a line of quadratically vanishing velocities off the Fermi surface along the k_x direction. The anomaly in the DOS is shown in the inset in Fig. 2 and numerically appears to behave roughly as -$|E|^{2/3}$ away from the peak. The behavior of $< v^{-1}(E) >$, whose importance is discussed below, is also shown, and is fit well with a $E^{-\frac{1}{4}}$ *divergence*.

The Fermi surface topology near the uBCP is given (for simplicity, scaling out the masses and the coefficient κ to get $\varepsilon_k = k_x^3 + k_y^2 - k_y^2$) from $\varepsilon_k = 0$ by

$$k_x = sgn(k_y^2 - k_z^2)|k_y^2 - k_z^2|^{1/3}. \quad (2)$$

This warped FS is displayed in Fig. 3 and is centered on the peculiar singular uBCP. As the uBCP is approached, the FS tangent plane becomes strongly dependent on the angle of approach, and the curvature becomes highly singular. Such a zero velocity point leads to arbitrarily low energy single-particle excitations around the uBCP on the FS, plus a "hot stripe" of low velocities just off the Fermi surface along the $\pm k_x$ axes whose impact on magnetic behavior may be crucial.

In Moriya's widely applied theory of nearly FM (and AF) metals, the inverse susceptibility has an imaginary part at low energy given by $N(E_F) < v^{-1} > \omega/q$. It is straightforward to show that when there is a BCP on a (non-vanishing) FS, $< v^{-1} >$ diverges. From Fig. 2, numerical scaling gives $< v^{-1}(E) > \sim E^{-1/4}$ for this uBCP. The divergence of this inverse moment of carrier velocity means that Moriya's theory as currently used breaks down, and requires generalization for the case of chemical potential approaching a BCP. At the BCP ($v_k \equiv 0$) a higher order expansion of the non-interacting susceptibility is required. If the

dispersion expansion Eq. 1 holds up to k_m (a few percent of the Brillouin zone dimension) we obtain (in the limit $\omega/Q^2 \to 0$ followed by $Q \to 0$)

$$\chi^\circ(Q,\omega) = \bar{\chi}^\circ(Q) + \sum_j \frac{f(\varepsilon_k) - f(\varepsilon_{k+Q})}{\varepsilon_{k+Q} - \varepsilon_k - \omega + i\eta} \to \sum_k \frac{\sum_j \frac{Q_j^2}{2m(k)_j}}{\sum_k \frac{Q_j^2}{2m(k)_j} - \omega + i\eta} \delta(\varepsilon_k), \qquad (3)$$

where the first term arises from $|\vec{k}| > k_m$ and is essentially that presented by SS, and the second term arises from the uBCP region. Here η is an infinitesimal and the masses $m(k)_j$ along the three axes are ($m_e\kappa/k_x$, m_y, -m_z). Neglecting the k_x dependence (which also changes sign) in the integrand for the real part will be a good approximation for $k < k_m$, and the bare fluctuation spectrum acquires a new kind of contribution from the region of the uBCP of

$$\Delta\chi^\circ(Q,\omega) \approx \Delta N(\varepsilon_F) \frac{Q_y^2/2m_y - Q_z^2/2m_z}{Q_y^2/2m_y - Q_z^2/2m_z - \omega} - i\pi\omega \sum_{k<k_m} \delta(\varepsilon_k)\delta(\frac{3k_x}{m_e\kappa} - [\frac{Q_y^2}{2m_y} - \frac{Q_z^2}{2m_z}]), (4)$$

Due to the different signs of the masses along y and z, the Q-dependent term in the denominator changes sign with the direction of $\vec{Q}$, hence the low energy magnetic fluctuation spectrum is highly anisotropic and is not a simple function of $\vec{Q}$ and ω. The damping (imaginary part) arises from the intersection of surfaces of constant k_x with the Fermi surface. Both are enhanced at the lowest energies by scattering processes involving the uBCP. This behavior replaces the conventional expansion $\chi^\circ(Q,\omega)^{-1} = \chi^\circ(0,0)^{-1} + AQ^2 - iC\omega/Q + ...)$, and it will be important to learn how interactions will renormalize this bare low energy behavior.

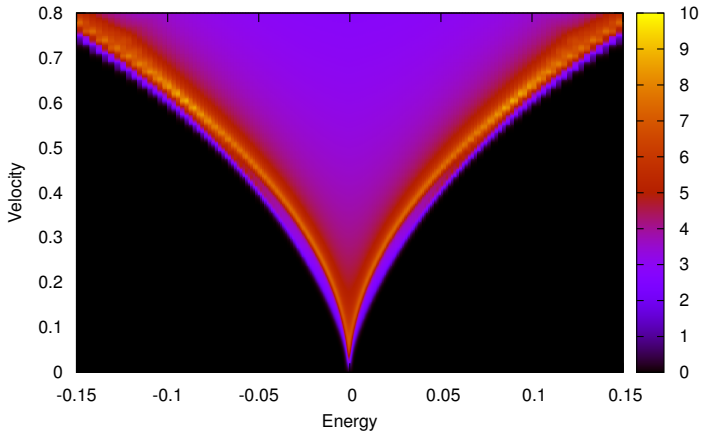

FIG. 5: Color plot representation of the velocity spectrum $D(\mathcal{E}, V)$, which provides the decomposition of velocities (vertical axis) for each energy (horizontal axis). All scales are arbitrary. The spectrum is sharply and narrowly peaked very near the onset, with a long tail at higher velocities.

Going beyond averages over the FS, the *spectrum* of carrier velocities (hence, single-particle and pair excitation energies) is of fundamental concern for spin fluctuations and

quantum criticality. We have evaluated the distribution of velocities V at energy $\mathcal{E}$ for the uBCP,

$$D(\mathcal{E}, V) = \sum_k \delta(\varepsilon_k - \mathcal{E})\delta(|\vec{v}_k| - V), \tag{5}$$

and displayed the results in Fig. 5. For isotropic free electrons this distribution vanishes except for a highly singular value along the line $V = \sqrt{2m\mathcal{E}}$, where it becomes the product of two δ-functions. The small V region of $D(\mathcal{E}, V)$ is sharply peaked in the vicinity of $V_m(E) = 3\mathcal{E}^{2/3}$, arising from the quadratically small velocity along the x-axis with relatively large phase space. The spectrum vanishes at smaller velocities $V < V_m$, but has a tail at higher velocities where the other two axes contribute.

So far we have only discussed the isolated uBCP, which would be most relevant to ferromagnetic, rather than antiferromagnetic, quantum criticality. In the hexagonal lattice there are six symmetry related such hot spots $Q_c(\pm 1, 0), Q_c(\pm\frac{1}{2}, \pm\frac{\sqrt{3}}{2})$, with $Q_c \approx 0.30$ Q_{zb} in terms of the zone boundary distance. There are therefore five non-zero Q-vectors spanning these hot spots, for which the large-Q susceptibility at zero or small energy will be correspondingly large, thus providing a driving force for spin-density waves (SDW) at the corresponding wavevectors. Note that, quite generally, the $q \to 0$ susceptibility approaches $\mathrm{N(E}_F)$, which also possesses a weak divergence at the BCP. Thus both FM and AF (SDW) susceptibilities will be strongly enhanced (hence competing); for transitions between inversion related hot-spots the SDW susceptibility will be particularly large, since the hot stripe axes will then be aligned.

Two other intermetallics, both with the cubic (C15) Laves structure rather than the hexagonal (C14) Laves structure of $NbFe_2$, have attracted much attention due to their weak magnetism. $TiBe_2$ at stoichiometry is a highly enhanced paramagnetic that was long believed to have weak order because magnetic order appears in impure samples. Van Hove singularities occur very near E_F; if non-stoichiometry moves E_F upward by as little at 3 meV, the velocity spectrum[23] $D(E_F, V)$ extends nearly to V=0 and $< v^{-1} >$ is enhanced by a factor of two, though there is no uBCP as in $NbFe_2$. Weak magnetism and metamagnetic transitions in $ZrZn_2$ have been attributed[19] to a saddle point van Hove singularity (a cBCP) very near E_F. The Ni_3Al (FM with small moment $< 0.1\mu_B/Ni$ below 40 K) and isovalent Ni_3Ga (highly enhanced but not ordered) pair have also attracted attention. The distinction was attributed by Aguayo *et al.*[24] to stronger spin fluctuations in Ni_3Ga, using analysis based on LDA results applied within Moriya theory. The band structure themselves are very similar except for one Al- (resp. Ga-)derived band, with no apparent anomaly in the band structure near E_F.

The $NbFe_2$ system, providing a rare example of itinerant, low temperature antiferromagnetism and non-Fermi liquid quasiparticle behavior at low temperature, seems to require a specific microscopic mechanism compared to the few other known weak itinerant magnets. We have proposed that an unconventional band critical point, in which an isolated point of vanishing carrier velocity on an extended Fermi surface, provides the explanation. Moriya's theory of weak magnetism requires generalization when the Fermi level lies near an uBCP, and the phenomenological renormalized Landau theory[25] that has been applied[26] to $ZrZn_2$ also must be generalized in this case. Generalizing the theory of itinerant quantum criticality to encompass such a uBCP should help to illuminate the mechanisms and the behavior around such itinerant QCPs.

We acknowledge K. Fredrickson who contributed to some of the calculations. This work was supported by DOE/SciDAC Grant No. DE-FC02-06ER25794 and by DOE grant DE-

FG02-04ER46111.

---

[1] M. Shiga and Y. Nakamura, J. Phys. Soc. Japan **56**, 4040 (1087).
[2] Y. Yamada and A. Sakata, J. Phys. Soc. Japan **57**, 46 (1088).
[3] M. Brando *et al.*, Physica B **378-380**, 111 (2006).
[4] M. Brando *et al.*, Phys. Rev. Lett. **101**, 026401 (2008).
[5] D. Moroni-Klementowicz, M. Brando, C. Albrecht, and F. M. Grosche, in *CP850, Low Temperature Physics: 24th Intl. Conf. on Low Temperature Physics*, eds. Y. Takano, S. P. Hershfield, S. O. Hill, P. J. Hirschfeld, and A. M. Goldman (AIP, 2006), p. 1251.
[6] A. J. Schofield, Phys. Stat. Sol. B **247**, 563 (2010).
[7] W. J. Duncan *et al.*, Phys. Stat. Sol. B **247**, 544 (2010).
[8] P. Coleman, Phys. Stat. Sol. B **247**, 506 (2010).
[9] J. Hertz, Phys. Rev. B **14**, 1165 (1976).
[10] A. J. Millis, Phys. Rev. B **48**, 7183 (1993).
[11] T. Moriya, *Spin Fluctuations in Itinerant Electron Magnetism*, (Springer, Berlin, 1985).
[12] G. G. Lonzarich and L. Taillefer, J. Phys. C **18**, 4339 (1985).
[13] M. Vojta, Rep. Prog. Phys. **66**, 2069 (2003).
[14] C. Pfleiderer, S. R. Julian, and G. G. Lonzarich, Nature **414**, 427 (2001).
[15] M. Imada, T. Misawa, and Y. Yamaji, J. Phys.: Condens. Matter **22**, 164206 (2010).
[16] M. R. Crook and R. Cywinski, Hyperfine Interactions **85**, 203 (1994).
[17] I. Dzyaloshinskii, J. Phys. I (France) **6**, 119 (1996).
[18] A. P. Kampf and A. A. Katanin, Phys. Rev. B **67**, 125104 (2003).
[19] Y. Yamaji, T. Misawa, and M. Imada, J. Phys. Soc. Japan **75**, 094719 (2006).
[20] N. Takayama and M.Shimizu, J. Phys. F: Met. Phys. **18**, L83 (1988).
[21] A. Subedi and D. J. Singh, Phys. Rev. B **81**, 024422 (2010); *erratum*, *ibid.* 059902(E) (2010).
[22] L. van Hove, Phys. Rev. **89**, 1189 (1953).
[23] T. Jeong, A. Kyker, and W. E. Pickett, Phys. Rev. B **73**, 115106 (2006).
[24] N. Aguayo, I. I. Mazin, and D. J. Singh, Phys. Rev. Lett. **94**, 147201 (2004).
[25] M. Shimizu, Rep. Prog. Phys. **44**, 329 (1981).
[26] I. I. Mazin and D. J. Singh, Phys. Rev. B **69**, 020402 (2004).